Lipid Modifications of a Ras Peptide Exhibit Altered Packing and Mobility versus Host Membrane as Detected by ^{2}H Solid-State NMR

Alexander Vogel,[†] Catherine P. Katzka,[‡] Herbert Waldmann,[‡] Klaus Arnold,[§]
Michael F. Brown,*[,||] and Daniel Huster*[,†,§]

Contribution from the Junior Research Group "Solid-State NMR Studies of Membrane-Associated Proteins", Biotechnological-Biomedical Center of the University of Leipzig, D-04107 Leipzig, Germany, Max Planck Institute of Molecular Physiology, D-44227 Dortmund, Germany, Institute of Medical Physics and Biophysics, University of Leipzig, D-04107 Leipzig, Germany, and Departments of Chemistry and Physics, University of Arizona, Tucson, Arizona 85721.

Received March 23, 2005; E-mail: mfbrown@u.arizona.edu; husd@medizin.uni-leipzig.de

Abstract: The human N-ras protein binds to cellular membranes by insertion of two covalently bound posttranslational lipid modifications, which is crucial for its function in signal transduction and cell proliferation. Mutations in ras may lead to unregulated cell growth and eventually cancer, making it an important therapeutic target. Here we have investigated the molecular details of the membrane binding mechanism. A heptapeptide derived from the C-terminus of the human N-ras protein was synthesized including two hexadecyl modifications. Solid-state ^{2}H NMR was used to determine the packing and molecular dynamics of the ras lipid chains as well as the phospholipid matrix. Separately labeling the chains of the peptide and the phospholipids with ^{2}H enabled us to obtain atomically resolved parameters relevant to their structural dynamics. While the presence of ras only marginally affected the packing of DMPC membranes, dramatically lower order parameters (S_{CD}) were observed for the ras acyl chains indicating modified packing properties. Essentially identical projected lengths of the 16:0 ras chains and the 14:0 DMPC chains were found, implying that the polypeptide backbone is located at the lipid−water interface. Dynamical properties of both the ras and phospholipid chains were determined from spin−lattice ^{2}H relaxation (R_{1Z}) measurements. Plots of R_{1Z} rates versus the corresponding squared segmental order parameters revealed striking differences. We propose the ras peptide is confined to microdomains containing DMPC chains which are in exchange with the bulk bilayer on the ^{2}H NMR time scale ($\sim 10^{-5}$ s). Compared to the host DMPC matrix, the ras lipid modifications are extremely flexible and undergo relatively large amplitude motions. It is hypothesized that this flexibility is a requirement for the optimal anchoring of lipid-modified proteins to cellular membranes.

Introduction

Posttranslational lipid modifications are a common structural motif of membrane-associated proteins and are responsible for their anchoring to the cell membrane.[1] In particular, proteins involved in signal transduction often feature this type of membrane anchor,[2] one prominent example being the G-Protein ras, which is also referred to as a GTPase. Such ras proteins are part of a signal transduction cascade responsible for cellular proliferation and differentiation.[3−5] Mutations in the protein may lead to uncontrolled cell growth, and ultimately cancer. It is known that up to 30% of all human cancers carry a mutated form of ras.[4] The structure of the soluble part of ras has been determined by X-ray diffraction[6] and solution NMR spectroscopy.[7] However, until recently little was known about the structure, dynamics, and details of the membrane association of the membrane binding C-terminus.

N-ras consists of 189 amino acids and has a molecular weight of ~21 kDa belonging to the important class of small guanine nucleotide binding proteins, including ADP ribosylation factors and other ras-related GTPases.[8] To date many investigations

[†] Biotechnological-Biomedical Center of the University of Leipzig.
[‡] Max Planck Institute of Molecular Physiology.
[§] Institute of Medical Physics and Biophysics, University of Leipzig.
[||] University of Arizona.

(1) (a) Clarke, S. *Annu. Rev. Biochem.* **1992**, *61*, 355−386. (b) Schafer, W. R.; Rine, J. *Annu. Rev. Genet.* **1992**, *26*, 209−237. (c) Schlesinger, M. J., Ed. *Lipid Modification of Proteins*; CRC Press: Boca Raton, FL, 1993.
(2) (a) Casey, P. J. *Science* **1995**, *268*, 221−225. (b) Gelb, M. H. *Science* **1995**, *275*, 1750−1751.
(3) Shields, J. M.; Pruitt, K.; McFall, A.; Shaub, A.; Der, C. J. *Trends Cell Biol.* **2000**, *10*, 147−154.
(4) Wittinghofer, A.; Waldmann, H. *Angew. Chem., Int. Ed.* **2000**, *39*, 4192−4214.

(5) (a) Reuther, G. W.; Der, C. J. *Curr. Opin. Cell Biol.* **2000**, *12*, 157−165. (b) Hall, A. *Science* **1994**, *264*, 1413−1414.
(6) Milburn, M. V.; Tong, L.; deVos, A. M.; Brünger, A.; Yamaizumi, Z.; Nishimura, S.; Kim, S. H. *Science* **1990**, *247*, 939−945.
(7) (a) Kraulis, P. J.; Domaille, P. J.; Campbell-Burk, S. L.; Van Aken, T.; Laue, E. D. *Biochemistry* **1994**, *33*, 3515−3531. (b) Krengel, U.; Schlichting, L.; Scherer, A.; Schumann, R.; Frech, M.; John, J.; Kabsch, W.; Pai, E. F.; Wittinghofer, A. *Cell* **1990**, *62*, 539−548. (c) Pai, E. F.; Kabsch, W.; Krengel, U.; Holmes, K. C.; John, J.; Wittinghofer, A. *Nature* **1989**, *341*, 209−214.
(8) Nie, Z.; Hirsch, D. S.; Randazzo, P. A. *Curr. Opin. Cell Biol.* **2003**, *15*, 396−404.

have shed light on the signal transduction cascade involving ras.[4,9] One reaction partner of ras is Sos which is responsible for its activation by catalyzing the release of guanosine diphosphate (GDP) from ras and subsequently the binding of guanosine triphosphate (GTP) resulting in its activation; ras then further affects downstream effectors. Mutated forms of ras are unable to hydrolyze GTP[10] and therefore cannot return to the deactivated state, which is believed to be connected to oncogenesis. Sos is bound to stimulated receptor tyrosine kinases via the protein Grb2 and thereby recruited from the cytoplasm to the membrane. Binding of proteins to the cell membrane increases their effective concentration by a factor of at least 1000.[11] The reaction rate between two partners is strongly increased by their localization at the membrane due to a higher apparent affinity;[12] if only one reaction partner is localized at the membrane the rate is largely unaffected. When ras is also bound to the membrane then a high reaction rate is followed by transduction of the signal. By contrast, if the membrane association of ras is disrupted then signal transduction is not observed. Thus, manipulation of the membrane association of ras plays an important regulatory role in controlling its function.

It has been shown that two posttranslational lipid modifications are necessary and sufficient to obtain the active form of ras.[13] In these posttranslational processing events, which target ras from the cytosol to the plasma membrane, the cysteine of the C-terminal −CAAX sequence (C is cysteine, A is an aliphatic amino acid, X is serine or methionine) is first farnesylated and then is recognized by a specific protease that cleaves the −AAX residues. Finally the new farnesylated cysteine at the C-terminus is converted to the methyl ester. In the case of N- and H-ras but not K-ras, the peptide chain is further modified by introduction of palmitic acid thioesters. [3−5] A single lipid modification apparently does not permanently anchor ras to the cell membrane.[14] Several biophysical studies have investigated the distribution of lipid-modified peptides between the membrane associated and the translocated cytosolic state.[11,15−19] It was found that the typical half-life for the membrane-associated state is on the order of seconds for singly lipidated peptides.[15,18] Addition of a second lipid modification increases the average half-life to the order of hours to days.[16,20] These conclusions are supported by the observation that singly lipid modified H-ras fails to activate mitogen-activated protein kinase (MAPK)[13] and that its activity is reduced by ∼98%.[21] In N-ras initially Cys[186] is farnesylated by a farnesyltransferase.

The second posttranslational modification is palmitoylation of Cys[181]; the cellular location where this reaction takes place is still under discussion. There are indications that the palmitoyltransferase is located at the cell membrane.[20,22] A kinetic trapping model postulates that the farnesylation is required to induce transient binding events that establish contacts between ras and the palmitoyltransferase.[23] Both transferases are possible targets for drug design, as ras is inactive when detached from the cell membrane. Inhibitors for farnesyltransferase have been found and tested with great success on mice and on human tumor cells in cell cultures.[24,25]

Currently, there is strong interest in understanding the mechanism of ras binding to the membrane via lipid modifications on account of their role in the development of cancer. In a previous study we determined the localization of the peptide within the lipid-water interface of the membrane.[26] Here we concentrate on molecular details of the lipid modifications anchoring the ras heptapeptide to the phospholipid membrane. Solid-state ^{2}H NMR is a powerful tool to determine motional parameters from line shape and relaxation rate analysis.[27−31] Moreover, the ^{2}H nucleus is well suited to study molecular dynamics by NMR, as it has very favorable properties for investigating molecular reorientations occurring over many orders of magnitude in time.[27−31] By application of a suitable motional model, details of the geometry of the molecular motion can be revealed from the ^{2}H NMR data. In particular, comprehensive models have been worked out for the motions of the acyl chains of the phospholipids in membranes.[28,32−35] More recently, ^{2}H NMR relaxation in combination with order parameter determination for the lipid chains has been successfully analyzed to determine elastic properties and deformations of lipid membranes.[36−39] We have applied this approach to a membrane-associated lipid-modified ras peptide. The ras hep-

(9) Hinterding, K.; Alonso-Diaz, D.; Waldmann, H. *Angew. Chem., Int. Ed.* **1998**, *37*, 688−749.
(10) Barbacid, M. *Annu. Rev. Biochem.* **1987**, *56*, 779−827.
(11) Murray, D.; Ben-Tal, N.; Honig, B.; McLaughlin, S. *Structure* **1997**, *5*, 985−989.
(12) Marshall, C. J. *Science* **1993**, *259*, 1865−1866.
(13) (a) Dudler, T.; Gelb, M. H. *J. Biol. Chem.* **1996**, *271*, 11541−11547. (b) Dudler, T.; Gelb, M. H. *Biochemistry* **1997**, *36*, 12434−12441.
(14) Silvius, J. R. In *Peptide−Lipid Interactions*; Simon, S. A., McIntosh, T. J., Eds. Elsevier: 2002; pp 371−395.
(15) Silvius, J. R.; l'Heureux, F. *Biochemistry* **1994**, *33*, 3014−3022.
(16) Shahinian, S.; Silvius, J. R. *Biochemistry* **1995**, *34*, 3813−3822.
(17) (a) Pool, C. T.; Thompson, T. E. *Biochemistry* **1998**, *37*, 10246−10255. (b) Janosch, S.; Nicolini, C.; Ludolph, B.; Peters, C.; Völkert, M.; Hazlet, T. L.; Gratton, E.; Waldmann, H.; Winter, R. *J. Am. Chem. Soc.* **2004**, *126*, 7496−7503.
(18) Peitzsch, R. M.; McLaughlin, S. *Biochemistry* **1993**, *32*, 10436−10443.
(19) Buser, C. A.; Sigal, C. T.; Resh, M. D.; McLaughlin, S. *Biochemistry* **1994**, *33*, 13093−13101.
(20) Schroeder, H.; Leventis, R.; Rex, S.; Schelhaas, M.; Nagele, E.; Waldmann, H.; Silvius, J. R. *Biochemistry* **1997**, *36*, 13102−13109.
(21) Bader, B.; Kuhn, K.; Owen, D. J.; Waldmann, H.; Wittinghofer, A.; Kuhlmann, J. *Nature* **2000**, *403*, 223−226.

(22) Liu, L.; Dudler, T.; Gelb, M. H. *J. Biol. Chem.* **1996**, *271*, 23269−23276.
(23) Dunphy, J. T.; Linder, M. E. *Biochim. Biophys. Acta* **1998**, *1436*, 245−261.
(24) Kohl, N. E.; Omer, C. A.; Conner, M. W.; Anthony, N. J.; Davide, J. P.; deSolms, S. J.; Giuliani, E. A.; Gomez, R. P.; Graham, S. L.; Hamilton, K. *Nat. Med.* **1995**, *1*, 792−797.
(25) Omer, C. A.; Kohl, N. E. *Trends Pharmacol. Sci.* **1997**, *18*, 437−444.
(26) Huster, D.; Vogel, A.; Katzka, C.; Scheidt, H. A.; Binder, H.; Dante, S.; Gutberlet, T.; Zschörnig, O.; Waldmann, H.; Arnold, K. *J. Am. Chem. Soc.* **2003**, *125*, 4070−4079.
(27) Davis, J. H. *Biochim. Biophys. Acta* **1983**, *737*, 117−171.
(28) Brown, M. F. *J. Chem. Phys.* **1982**, *77*, 1576−1799.
(29) (a) Vold, R. R.; Vold, R. L. In *Advances in Magnetic and Optical Resonance*; Warren, W. S., Ed.; Academic Press: San Diego, CA, 1991; pp 85−171. (b) Vold, R. R. In *Nuclear Magnetic Resonance Probes of Molecular Dynamics*; Tycko, R., Ed. Kluwer Academic Publishers: Dodrecht, 1994; pp 27−112. (c) Wittebort, R. J.; Olejniczak, E. T.; Griffin, R. G. *J. Phys. Chem.* **1987**, *86*, 5411−5420.
(30) Seelig, J. *Q. Rev. Biophys.* **1977**, *10*, 353−418.
(31) (a) Seelig, J.; Seelig, A. *Q. Rev. Biophys.* **1980**, *13*, 19−61. (b) Gröbner, G.; Burnett, I. J.; Glaubitz, C.; Choi, G.; Mason, A. J.; Watts, A. *Nature* **2000**, *405*, 810−813. (c) Nevzorov, A. A.; Moltke, S.; Heyn, M. P.; Brown, M. F. *J. Am. Chem. Soc.* **1999**, *121*, 7636−7643. (d) Nevzorov, A. A.; Moltke, S.; Brown, M. F. *J. Am. Chem. Soc.* **1998**, *120*, 4798−4805.
(32) Brown, M. F. In *Biological Membranes. A Molecular Perspective from Computation and Experiment*; Merz, K. M., Roux, B., Eds.; Birkhäuser: Boston, 1996; pp 175−252.
(33) Petrache, H. I.; Dodd, S. W.; Brown, M. F. *Biophys. J.* **2000**, *79*, 3172−3192.
(34) Nevzorov, A. A.; Trouard, T. P.; Brown, M. F. *Phys. Rev. E.* **1998**, *58*, 2259−2281.
(35) Trouard, T. P.; Alam, T. M.; Brown, M. F. *J. Chem. Phys.* **1994**, *101*, 5229−5261.
(36) Otten, D.; Brown, M. F.; Beyer, K. *J. Phys. Chem. B* **2000**, *104*, 12119−12129.
(37) Brown, M. F.; Thurmond, R. L.; Dodd, S. W.; Otten, D.; Beyer, K. *J. Am. Chem. Soc.* **2002**, *124*, 8471−8484.
(38) Brown, M. F.; Thurmond, R. L.; Dodd, S. W.; Otten, D.; Beyer, K. *Phys. Rev. E.* **2001**, *64*, 010901.
(39) Martinez, G. V.; Dykstra, E. M.; Lope-Piedrafita, S.; Job, C.; Brown, M. F. *Phys. Rev. E.* **2002**, *66*, 050902.

Scheme 1. Lipidated ras and ras-d_{66} Peptides

H-Gly-Cys(R_2)-Met-Gly-Leu-Pro-Cys(R_1)-OMe

ras peptide: R_1=HD, R_2=Pal
ras-d_{66} peptide: R_1=HD-d_{33}, R_2=HD-d_{33}

tapeptide contains two thioether-linked hexadecyl chains, which are either deuterated for ^{2}H NMR investigations in a nondeuterated host matrix or protiated for ^{2}H NMR studies of their influence on a deuterated DMPC host matrix. Thus, by switching the ^{2}H label between the peptide and the host membrane, structural data and elastic properties for either component of the system have been analyzed in detail. Our work reveals that the ras hydrocarbon and the DMPC acyl chains are closely matched in their projected length along the normal to the bilayer surface. Interestingly, the microdomains containing ras chains are extremely flexible and exhibit the properties of phospholipid acyl chains in the presence of a detergent. Our work represents the first comprehensive dynamical study of the posttranslational lipid modifications of a membrane-associated peptide, providing insight into the molecular details of the mechanism of protein binding to cellular membranes linked to oncogenesis.

Experimental Procedures

Materials. The glycerophospholipids 1,2-dimyristoyl-*sn*-glycero-3-phosphocholine (DMPC) and 1,2-diperdeuteriomyristoyl-*sn*-glycero-3-phosphocholine (DMPC-d_{54}) as well as cholesterol were procured from Avanti Polar Lipids, Inc. (Alabaster, AL) and used without further purification. The nonionic detergent octaethyleneglycol-mono-*n*-dodecyl ether ($C_{12}E_8$) was obtained from Fluka (Taufkirchen, Germany). Protected amino acids and coupling reagents were obtained from Novabiochem (La Jolla, CA) and ^{2}H$_{33}$-labeled hexadecyl alcohol was from Isotec (Miamisburg, OH).

Peptide Synthesis. The ras peptide with the amino acid sequence H-Gly-Cys(R^1)-Met-Gly-Leu-Pro-Cys(R^2)-OMe was synthesized following references[9,40,41] (see Supporting Information) where R^1 and R^2 indicate the lipid modifications. In the protiated ras peptide R^1 represents a palmitoyl (Pal) thioester and R^2 is a hexadecyl (HD) thioether modification; for the deuterated ras peptide, we chose to substitute the palmitoyl thioester with a more stable thioether due to the limited availability of the perdeuterated palmitoyl-d_{33} chloride. Both R^1 and R^2 are perdeuterated hexadecyl-d_{33} thioether modifications. In the following, these peptides are abbreviated as ras and ras-d_{66}, respectively (Scheme 1).

Sample Preparation. Aliquots of phospholipid and peptide, phospholipid and cholesterol, or phospholipid and $C_{12}E_8$ (molar ratios of 10:1, 1:1, and 2:1, respectively) were combined in chloroform, dried under a stream of nitrogen, and then dissolved in cyclohexane. After freezing in liquid nitrogen, the samples were lyophilized under a vacuum of approximately 0.1 mbar. Subsequently, the sample was hydrated to 40−50 wt % (90 wt % for DMPC-d_{54}/$C_{12}E_8$) with deuterium-depleted ^{1}H$_2$O, freeze−thawed, stirred, and gently centrifuged for equilibration. They were then transferred to 5-mm glass vials and finally sealed with a plastic cap and Parafilm for NMR measurements. Mixtures of DMPC-d_{54} and $C_{12}E_8$ at a molar ratio of 2:1, a water content of 90 wt %, and a temperature of 40 °C are known to spontaneously align in magnetic fields.[36] We exploited this effect to obtain better spectral resolution.

Deuterium Solid-State NMR Spectroscopy. ^{2}H NMR spectra were acquired with a widebore Bruker Avance 750 NMR spectrometer operating at a resonance frequency of 115.1 MHz for ^{2}H (magnetic

field strength of 17.6 T). A single-channel solids probe equipped with a 5-mm solenoid coil was used. The ^{2}H NMR spectra were accumulated with a spectral width of ±250 kHz using quadrature phase detection, a phase-cycled quadrupolar echo sequence[42] with two 3.0 μs π/2 pulses separated by a 60 μs delay, and a relaxation delay of 1 s. A phase-cycled inversion−recovery quadrupolar echo pulse sequence was used to measure the relaxation times for the decay of Zeeman order (T_{1Z}; spin−lattice relaxation time). A relaxation delay of 2 s was used, and all other parameters were the same as those for recording the ^{2}H NMR spectra. The signals were left-shifted after acquisition to initiate the Fourier transformation beginning at the top of the quadrupolar echo. Only data from the real channel were processed to yield symmetrized ^{2}H NMR spectra; an exponential line broadening not exceeding 50 Hz was applied.

The ^{2}H NMR powder-type spectra were de-Paked[43] using the algorithm of McCabe and Wassall,[44] and order parameter profiles were determined from the observed quadrupolar splittings ($\Delta\nu_Q$) according to

$$|\Delta\nu_Q^{(i)}| = \frac{3}{2}\chi_Q|S_{CD}^{(i)}||P_2(\cos\theta)| \tag{1}$$

Here $\chi_Q = e^2qQ/\hbar$ represents the quadrupolar coupling constant (167 kHz for ^{2}H in the C−^{2}H bond), $S_{CD}^{(i)} = {}^1/_2\langle 3\cos^2\beta_i - 1\rangle$ is the segmental order parameter, θ is the angle between the bilayer director axis and the main external magnetic field, and P_2 is the second Legendre polynomial. For the de-Paked ^{2}H NMR spectra $\theta = 0°$ and hence $P_2(\cos\theta) = 1$. Details of the order parameter determination have been described before.[45] The Pake doublets have been assigned starting at the terminal methyl group, which exhibits the smallest quadrupolar splitting. The methylene groups were assigned consecutively according to their increasing quadrupolar splittings.

Theoretical Background

Calculation of Structural Parameters Using Mean Torque Model. The ^{2}H NMR spectra of powder-type or oriented samples enable the order parameters of the ^{2}H labeled segments to be obtained using eq 1. From the $S_{CD}^{(i)}$ order profiles the average area per hydrocarbon chain $\langle A\rangle$, the thickness of the hydrocarbon region D_C, and the average position of each carbon segment i along the bilayer normal $\langle z_i\rangle$ can be calculated. The most important value for calculating the structural parameters is the instantaneous travel of each carbon segment i along the bilayer normal D_i, which can have a maximum value of $D_M = 2.54$ Å. It is defined by the projection of the vector connecting the two neighboring carbons of the segment i onto the bilayer normal[33]

$$D_i = D_M\cos\beta_i = z_{i-1} - z_{i+1} \tag{2}$$

where β_i is the angle between the vector connecting the neighboring carbons and the bilayer normal. The average travel of the carbon segment i along the bilayer normal can be calculated from

$$\langle D_i\rangle = D_M\langle\cos\beta_i\rangle = \langle z_{i-1}\rangle - \langle z_{i+1}\rangle \tag{3}$$

where the brackets denote an ensemble or time average. Note that eqs 2 and 3 imply that D_i is twice the travel of one methylene group. The values for the average positions of the different carbon segments also enable calculation of the average

(40) Nägele, E.; Schelhaas, M.; Kuder, N.; Waldmann, H. *J. Am. Chem. Soc.* **1998**, *120*, 6889−6902.
(41) Schelhaas, M.; Glomsda, S.; Hänsler, M.; Jakubke, H.-D.; Waldmann, H. *Angew. Chem., Int. Ed. Engl.* **1996**, *35*, 106−109.

(42) Davis, J. H.; Jeffrey, K. R.; Bloom, M.; Valic, M. I.; Higgs, T. P. *Chem. Phys. Lett.* **1976**, *42*, 390−394.
(43) Sternin, E.; Bloom, M.; MacKay, L. *J. Magn. Reson.* **1983**, *55*, 274−282.
(44) McCabe, M. A.; Wassall, S. R. *J. Magn. Reson. B* **1995**, *106*, 80−82.
(45) Huster, D.; Arnold, K.; Gawrisch, K. *Biochemistry* **1998**, *37*, 17299−17308.

projected chain length $\langle L_C^* \rangle$ via

$$\langle L_C^* \rangle = \langle z_2 \rangle - \langle z_{n_C} \rangle = \sum_{i=3,5\ldots}^{n_C-1} \langle D_i \rangle \quad (4)$$

Here n_C is the number of carbons per chain, and the average projected chain length is defined as the distance between the second carbon and the terminal methyl group.

On the other hand, the structural parameters $\langle A \rangle$ and D_C are calculated from the values obtained just for the plateau region carbon segments.[33] Here, the case of two identical hydrocarbon chains is treated. Making the assumption that the hydrocarbon chains have the shape of a cylinder or cuboid, the average cross-sectional area for both hydrocarbon chains can be expressed by

$$\langle A \rangle = \frac{4V_{CH_2}}{D_M}\left\langle \frac{1}{\cos\beta} \right\rangle \quad (5)$$

where V_{CH_2} is the volume of a single methylene group. For disaturated lipids the volume of a single methylene group V_{CH_2}, which is a function of absolute temperature T, can be approximated by $V_{CH_2}(T) \approx V_{CH_2}{}^0 + \alpha_{CH_2}(T - 273.15\ \text{K})$, with the empirical parameters $V_{CH_2}{}^0 = 26.5\ \text{Å}^3$ and $\alpha_{CH_2} = 0.0325$ $\text{Å}^3/\text{K}$. For the calculation of eq 5, the value of $\langle 1/\cos\beta \rangle$ is also needed, which can be approximated by[33]

$$\left\langle \frac{1}{\cos\beta} \right\rangle \approx 3 - 3\langle\cos\beta\rangle + \langle\cos^2\beta\rangle \quad (6)$$

If the hydrocarbon chain has the shape of a cylinder or cuboid then the hydrocarbon thickness D_C is related to $\langle A \rangle$ by

$$D_C = \frac{2V_C}{\langle A \rangle} \quad (7)$$

where V_C is the volume of a single hydrocarbon chain. Assuming that the methyl volume is twice the methylene volume, $V_{CH_3} \approx 2V_{CH_2}$, D_C can be expressed using eqs 5 and 7 by

$$D_C = \frac{1}{2}n_C D_M \left\langle \frac{1}{\cos\beta} \right\rangle^{-1} \quad (8)$$

Now, for the calculation of $\langle z_i \rangle$ by means of eq 3, $\langle A \rangle$ using eqs 5 and 6, and D_C in terms of eqs 6 and 8, one needs the values of the moments $\langle \cos\beta_i \rangle$ and $\langle \cos^2\beta_i \rangle$. They can be obtained from the measured $S_{CD}^{(i)}$ order parameters. The calculation of $\langle \cos^2\beta_i \rangle$ is straightforward and is given by

$$\langle \cos^2\beta_i \rangle = \frac{1 - 4S_{CD}^{(i)}}{3} \quad (9)$$

However, the calculation of $\langle \cos\beta_i \rangle$ is more complicated since $\langle \cos^2\beta_i \rangle^{1/2} \neq \langle \cos\beta_i \rangle$. To correlate $\langle \cos\beta_i \rangle$ with $\langle \cos^2\beta_i \rangle$ a model describing the population of all possible tilt angles β_i is required. For a model in terms of a mean torque, the distribution function $f_i(\beta_i)$ describing this population is defined by

$$f_i(\beta_i) = \frac{1}{Z_i}\exp\left(-\frac{U_i(\beta_i)}{k_B T}\right) \quad (10)$$

where the partition function is

$$Z_i = \int_0^\pi \exp\left(-\frac{U_i(\beta_i)}{k_B T}\right)\sin\beta_i\,\mathrm{d}\beta_i \quad (11)$$

Here the distribution function as well as the partition function are generated by the potential of mean torque $U_i(\beta_i)$, which in a first-order approximation is given by[33]

$$U_i(\beta_i) \approx U_i \cos\beta_i \quad (12)$$

Using this framework, an analytical solution for $\langle \cos\beta_i \rangle$ can be obtained by applying the approximation $\coth(-U_i/k_B T) \approx 1$ leading to[46]

$$\langle \cos\beta_i \rangle = \frac{1}{2}\left(1 + \sqrt{\frac{-8S_{CD}^{(i)} - 1}{3}}\right) \quad (13)$$

This equation is only applicable to certain values of the order parameters, as the radicand is real only for $S_{CD}^{(i)} \leq -1/8$, with relatively high deviations for values close to $S_{CD}^{(i)} \approx -1/8$. To calculate $\langle \cos\beta_i \rangle$ for smaller order parameters, one can numerically solve the following coupled equations:

$$\langle \cos\beta_i \rangle = \frac{1}{Z_i}\int_{-1}^1 \cos\beta_i \exp\left(\frac{-U_i\cos\beta_i}{k_B T}\right)\mathrm{d}\cos\beta_i = $$
$$\coth\left(\frac{-U_i}{k_B T}\right) + \frac{k_B T}{U_i} \quad (14)$$

$$\langle \cos^2\beta_i \rangle = \frac{1}{Z_i}\int_{-1}^1 \cos^2\beta_i \exp\left(\frac{-U_i\cos\beta_i}{k_B T}\right)\mathrm{d}\cos\beta_i = $$
$$1 + 2\left(\frac{-k_B T}{U_i}\right)^2 + \frac{2k_B T}{U_i}\coth\left(\frac{-U_i}{k_B T}\right) \quad (15)$$

The first-order model for the mean-torque potential used for the calculations in this article has been shown to be superior to other descriptions such as the diamond lattice model.[33]

Results

^{2}H NMR Spectra and Order Parameter Profiles. In this work we have compared the properties of the acyl chains in three different samples: (i) pure DMPC-d_{54}, (ii) DMPC-d_{54}/ras at a 10:1 molar ratio, and (iii) DMPC/ras-d_{66} at a 10:1 molar ratio. Thus, structural and dynamical information about the ras hydrocarbon chains in comparison to the phospholipid chains can be extracted from the ^{2}H NMR data. Furthermore, this combination of samples allows one to determine the effect of the ras peptide on the bilayer properties of the host DMPC matrix. Although the lipid to peptide molar ratio is relatively low, from our previous studies we have no indication for peptide aggregation.[26,48] We have used magic-angle spinning to detect the high-resolution ^{1}H NMR spectrum of the ras peptide in a perdeuterated lipid matrix under identical conditions. The ^{1}H NMR spectra showed very good resolution suggesting that the peptide is highly mobile in the lipid membrane. Since the ras peptide provided ^{1}H MAS NMR line widths that are only

(46) Petrache, H. I.; Tu, K.; Nagle, J. F. *Biophys. J.* **1999**, *76*, 2479−2487.
(47) (a) Koenig, B. W.; Strey, H. H.; Gawrisch, K. *Biophys. J.* **1997**, *73*, 1954−1966. (b) Petrache, H. I.; Tristram-Nagle, S.; Nagle, J. F. *Chem. Phys. Lipids* **1998**, *95*, 83−94.
(48) Huster, D.; Kuhn, K.; Kadereit, D.; Waldmann, H.; Arnold, K. *Angew. Chem., Int. Ed.* **2001**, *40*, 1056−1058.
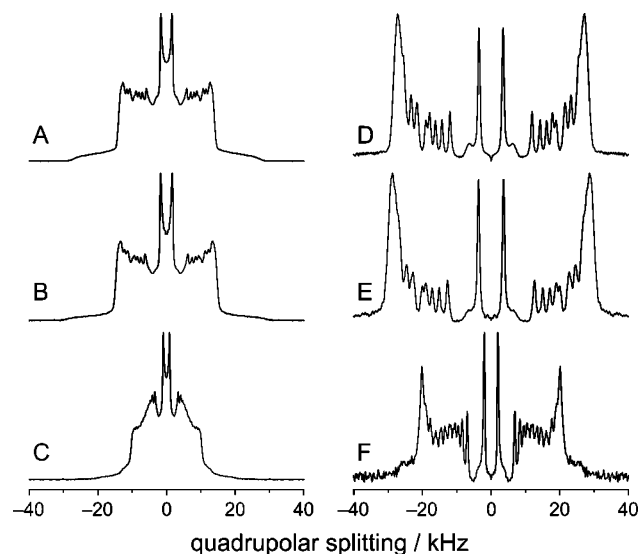
Figure 1. Representative solid-state ^{2}H NMR spectra of (A) DMPC-d_{54}, (B) DMPC-d_{54}/ras (10:1 mol/mol), and (C) DMPC/ras-d_{66} (10:1 mol/mol) in the L_α phase recorded at a temperature of 30 °C. The samples contained 40 wt % deuterium-depleted ^{1}H$_2$O. The corresponding de-Paked ^{2}H NMR spectra are shown in parts D−F.

Figure 2. Profiles of the segmental order parameter $|S_{CD}^{(i)}|$ as a function of reverse chain segment index i where the position of the terminal methyl group is designated as ω. Data are shown for DMPC-d_{54} (○), DMPC-d_{54}/ras (10:1 mol/mol) (●), and DMPC/ras-d_{66} (10:1 mol/mol) (▲). Note that the order parameters of ras-d_{66} are much smaller than those of DMPC-d_{54} which remain almost unchanged upon binding of the peptide.

Table 1. Summary of Structural Results for DMPC-d_{54}, DMPC-d_{54}/ras, and DMPC/ras-d_{66} in the Liquid−Crystalline (L_α) State at 30 °C

	$\langle A \rangle /\text{Å}^{2\ a}$	$D_C/\text{Å}^b$	$\langle L_C^* \rangle /\text{Å}^c$
DMPC-d_{54}	59.5	12.9	10.1
DMPC-d_{54}/ras^d	58.3	13.2	10.3
DMPC/ras-d_{66}^{d}	67.0	13.1	10.1

^{a} Cross-sectional area of both hydrocarbon chains (eq 5). ^{b} Volumetric hydrocarbon thickness (eq 8). ^{c} Chain extent (eq 4). ^{d} 10:1 molar ratio.

slightly broader than those of the phospholipids, we concluded that the ras peptide is well incorporated in the membrane as a monomer.

In Figure 1A−C, ^{2}H NMR powder-type spectra of randomly oriented multilamellar samples of DMPC-d_{54}, DMPC-d_{54}/ras, and DMPC/ras-d_{66} at a temperature of 30 °C are shown. All spectra show good resolution with several resolved sets of quadrupolar splittings. Striking differences between the ^{2}H NMR spectra of DMPC-d_{54} and ras-d_{66} are observed. It is noteworthy that the spectrum of ras-d_{66} is much narrower than that of DMPC-d_{54}. This indicates that the order parameters of the ras peptide are much lower than those of DMPC. However, the differences between DMPC-d_{54} in the presence and absence of ras peptide are rather small, the main difference being that the ^{2}H NMR spectrum in the presence of ras peptide is slightly wider indicating slightly higher order parameters.

Note that in Figure 1 the ^{2}H NMR spectra consist of a superposition of multiple Pake doublets, which can be assigned to the different carbon segments of the deuterated acyl chains.[30] A Pake doublet shows an orientation dependence described by the second Legendre polynomial $P_2(\cos \beta)$ weighted by a random spherical powder distribution. These Pake doublets can be deconvoluted using a numerical inversion procedure (called "de-Pakeing"),[43] which calculates an oriented spectrum at a certain sample orientation. In the case of the $\theta = 0°$ sample orientation this results in a spectrum with considerably improved spectral resolution, illustrated by Figure 1 D−F. In principle, the same observations as for the powder-type spectra can be made, which are facilitated by the improvement in the spectroscopic separation of different quadrupolar splittings by de-Pakeing. Each of the separated quadrupolar splittings can be converted into order parameters using eq 1.

Order parameter profiles of DMPC-d_{54}, DMPC-d_{54}/ras, and DMPC/ras-d_{66} showing the dependence on the position of the carbon segment in the acyl chain are presented in Figure 2. The segments are numbered consecutively starting at the carbonyl group of the lipid or the carbon directly connected to the sulfur
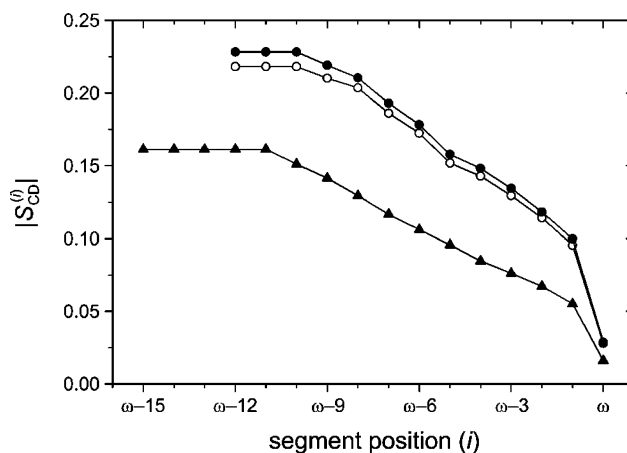
atom of the cysteine residues of the ras peptide, respectively. The assumption was made that the order parameters decrease monotonically for the carbon segments proceeding toward the terminal methyl group of the chain. As can be seen, the order profiles for DMPC-d_{54} in the presence and absence of ras peptide are very similar. The only differences are the slightly higher order parameters in the presence of the ras peptide, indicating that it influences the surrounding lipids only to a very small extent. It is striking that the order parameter profile for ras-d_{66} in a DMPC matrix is quite different. Dramatically lower absolute order parameters are calculated from the narrower spectrum of the ras-d_{66} chains. This indicates that the hydrocarbon chains of the ras peptide occupy a substantially greater conformational space than the DMPC hydrocarbon chains.

It is worth recalling that the upper end of the chains comprises a region where the order parameter values of the different carbon segments are very close to one another. In the ^{2}H NMR spectra this results in large peaks corresponding to a high quadrupolar splitting, encompassing a superposition of several Pake doublets belonging to methylene groups close to the glycerol or peptide backbone, respectively. This region is called the plateau region, and the obtained order parameter is used for calculation of the average area per hydrocarbon chain $\langle A \rangle$ and the thickness of the hydrocarbon region D_C (vide infra).

Determination of Interfacial Molecular Areas, Hydrocarbon Thicknesses, and Projected Chain Lengths Using the Mean-Torque Model. The values of $\langle A \rangle$, D_C, and $\langle L_C^* \rangle$ calculated for DMPC-d_{54} in the presence and absence of ras and for ras-d_{66} in a DMPC matrix are summarized in Table 1. The hydrocarbon thickness for DMPC-d_{54} is in good agreement with the values observed by X-ray scattering.[47] The higher absolute

Table 2. Segmental Order Parameters $|S_{CD}^{(i)}|$ and Spin−Lattice Relaxation Rates $R_{1Z}^{(i)}$ for DMPC-d_{54}, DMPC-d_{54}/ras, and DMPC/ras-d_{66} Obtained at a Magnetic Field Strength of 17.6 T (115.1 MHz) at 30 °C

acyl chain segment	DMPC-d_{54}[a]		DMPC-d_{54}/ras[a,b]		acyl chain segment	DMPC/ras-d_{66}[a,b]	
	$\|S_{CD}^{(i)}\|$	$R_{1Z}^{(i)}$/s^{-1}	$\|S_{CD}^{(i)}\|$	$R_{1Z}^{(i)}$/s^{-1}		$\|S_{CD}^{(i)}\|$	$R_{1Z}^{(i)}$/s^{-1}
					1−5	0.1613	32.39
2−4	0.2182	26.82	0.2283	28.34	6	0.1512	26.35
5	0.2102	24.11	0.2191	22.91	7	0.1415	26.41
6	0.2036	21.67	0.2105	20.02	8	0.1294	23.11
7	0.1861	18.15	0.1930	19.09	9	0.1166	26.16
8	0.1724	15.87	0.1782	16.16	10	0.1062	24.11
9	0.1519	15.76	0.1578	16.36	11	0.0958	25.22
10	0.1429	14.39	0.1482	14.01	12	0.0846	22.00
11	0.1294	11.39	0.1344	11.02	13	0.0763	16.27
12	0.1142	8.70	0.1183	8.48	14	0.0673	13.89
13	0.0955	10.20	0.0999	11.19	15	0.0553	10.23
14	0.0279	3.18	0.0287	3.17	16	0.0160	3.23

[a] 50 wt % $^{1}H_2O$. [b] 10:1 molar ratio.

magnitudes of the order parameters of DMPC-d_{54} in the presence of the ras peptide indicate a slightly thicker hydrocarbon core, so that the interfacial area per chain is somewhat smaller compared to pure DMPC-d_{54}. For ras-d_{66} in a DMPC matrix the hydrocarbon thickness is very close to the values for DMPC-d_{54}, while the average area per hydrocarbon chain is much larger. This is in good agreement with our former investigations, which also showed ras and DMPC to have very similar hydrocarbon chain lengths.[26] This chain length matching is not a result of a tilt of the ras acyl chains since no transverse order is observed in FTIR studies (results not shown). Furthermore, a tilt would lead to an increase in the ^{2}H NMR order parameters that is not observed. In fact, the large cross-sectional area of the ras hydrocarbon chains and the matching to the projected length of the DMPC chains is caused by their strong tendency to disorder. The large cross-sectional area of the ras chains provide space for the peptide backbone that occupies a substantial area in the lipid−water interface. The free volume in the membrane core is "filled" by the hydrophobic peptide side chains Leu and Met[26] and by the large amplitude motions of the ras lipid chains covalently bound to the Cys residues. Therefore, the matching of the length of the ras hydrocarbon chains is a result of several interactions: first, energetically favorable hydrophobic contacts between the hydrocarbon chains of the ras peptide and DMPC and, second, the accommodation of the interfacial area of the ras hydrocarbon chains to the area that the peptide backbone occupies in the lipid−water interface.

Values of the segmental order parameters are plotted in Figure 2, and the numerical values are provided in Table 2. These quantities can be used to calculate the average positions of the carbon segments along the bilayer normal starting from the terminal methyl group, for which the position $\langle z_{n_C} \rangle$ is set to zero. The resulting chain extension profiles are shown in Figure 3. Again, the difference between DMPC-d_{54} in the presence and in the absence of ras peptide is barely noticeable. However, for the 16:0 chains of ras-d_{66} in a DMPC matrix the slope of the chain extension profile is dramatically altered. Our analysis leads to the remarkable conclusion that the average distance between the C-2 carbon segment in the beginning of the chain and the methyl end $\langle L_C^* \rangle$ is very close for all three samples, despite that a single ras-d_{66} hydrocarbon chain contains two additional
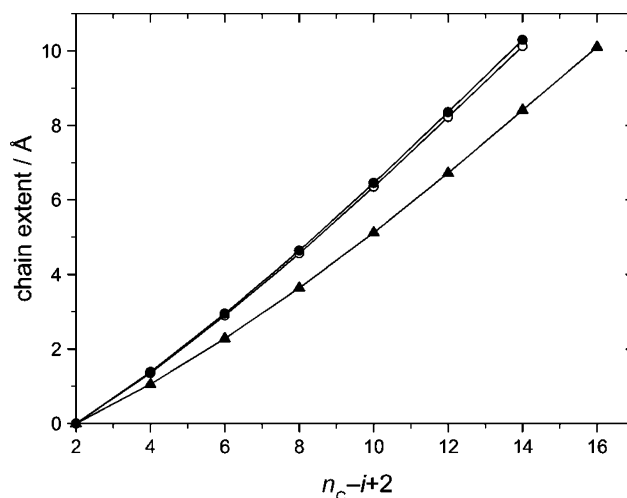

Figure 3. Chain extension profiles showing the cumulative projection of the acyl segments onto the bilayer normal. The average distance of the carbon i from the terminal methyl group ($i = n_C$) is shown for DMPC-d_{54} (○), DMPC-d_{54}/ras (10:1 mol/mol) (●), and DMPC/ras-d_{66} (10:1 mol/mol) (▲). The indexing of the chain is identical to Figure 2 where the terminal methyl group corresponds to $n_C - i + 2 = 2$ and is at the origin. Although the hydrocarbon chains of ras-d_{66} each contain two additional methylene groups versus the DMPC-d_{54} chains, the distance between the C-2 carbon and the terminal methyl group is almost the same in each case.

methylene groups compared to a DMPC-d_{54} acyl chain. This is in good agreement with the observation that the thickness of the hydrocarbon core of the membrane is very similar for all three samples (Table 1). The deviation of the ras-d_{66} chains from the packing curves of the DMPC matrix is a characteristic feature of the former system. It has been shown previously that membranes composed of identical phospholipid species with varying hydrocarbon chain lengths fall exactly on the same packing curve exhibiting the same chain extension profiles.[33] By contrast, phospholipids with different headgroups exhibit modified slopes in these plots. Specifically phospholipids with smaller headgroups exhibit steeper slopes in the chain extension profiles.[33]

Investigation of Chain Molecular Dynamics by ^{2}H Relaxation. To provide dynamic information, ^{2}H NMR spin−lattice relaxation (T_{1Z}) measurements were performed for the various samples studied. The inverse of the relaxation time defines the spin−lattice relaxation rate R_{1Z}, which is also summarized for the various hydrocarbon chain segments in Table 2. In Figure 4 the dependence of the relaxation rate on the segment position is plotted. The relaxation rates for ras-d_{66} are generally higher than those for DMPC-d_{54}. The differences are particularly pronounced in the lower middle region of the chains, whereas they are smaller at the beginning and the end of the chains. Remarkably, the dynamic properties of DMPC seem to be barely influenced by the incorporation of the ras peptide.

In previous analyses of pure phospholipid membranes, it has been found that the relaxation rate often exhibits a linear dependence on the square of the order parameter.[28,34,35,49] While the physical reason for this interesting behavior is still under discussion, it has been shown to be a common feature for disaturated phospholipids. The square-law plots for DMPC-d_{54} in the presence and absence of the ras peptide as well as for ras-d_{66} in a DMPC matrix are shown in Figure 5. For

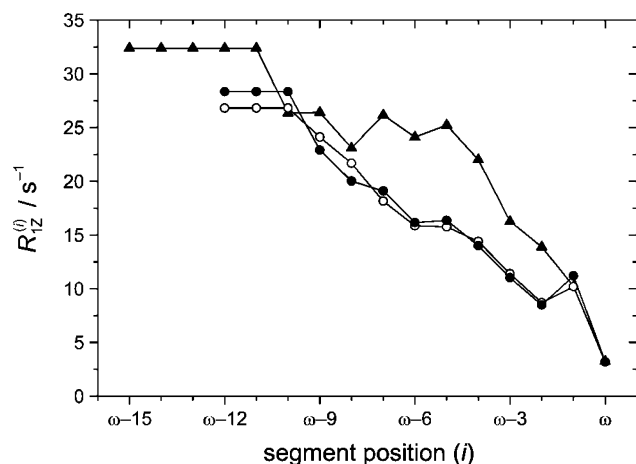(49) Brown, M. F.; Ribeiro, A. A.; Williams, G. D. *Proc. Natl. Acad. Sci. U.S.A.* **1983**, *80*, 4325−4329.

Figure 4. Profiles of spin−lattice relaxation rates $R_{1Z}^{(i)}$ as a function of reverse chain segment index i where the position of the terminal methyl group is designated as ω. Data obtained for powder-type samples at 115.1 MHz (17.6 T) are shown: DMPC-d_{54} (○), DMPC-d_{54}/ras (10:1 mol/mol) (●), and DMPC/ras-d_{66} (10:1 mol/mol) (▲). While the relaxation rates of DMPC-d_{54} remain almost unchanged upon binding of the peptide, the relaxation rates for ras-d_{66} are generally higher.
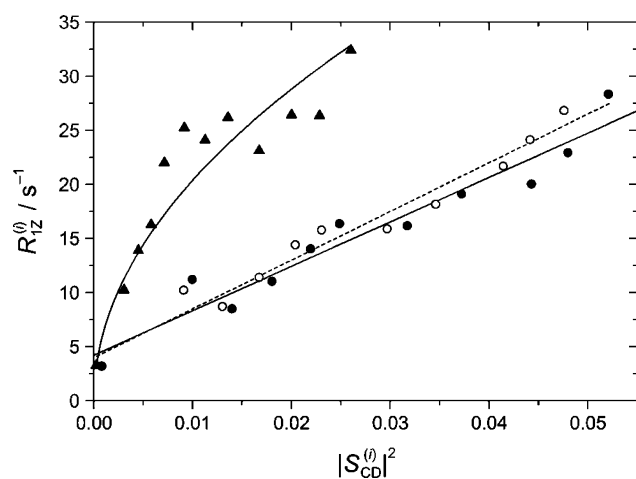

Figure 5. Dependence of $R_{1Z}^{(i)}$ rates on the corresponding order parameter squared for DMPC-d_{54} (○), DMPC-d_{54}/ras (10:1 mol/mol) (●), and DMPC/ras-d_{66} (10:1 mol/mol) (▲) at 115.1 MHz (17.6 T). Lines are drawn to guide the eye. Assuming the relaxation is governed by order fluctuations, the flexibility of DMPC-d_{54} is almost unchanged upon binding of ras, while ras itself exhibits a much larger flexibility.

DMPC-d_{54} in the presence as well as in the absence of ras peptide, the dependence is linear which is in good agreement with the previously obtained data. However, the $R_{1Z}^{(i)}$ versus $|S_{CD}^{(i)}|^2$ plot for the ras-d_{66} hydrocarbon chains departs from the linear dependence and shows a bent shape with a steeper slope. Previous investigations of phospholipids have shown that the slope of the square law plots is correlated with the elastic properties of the membranes.[34,35,49] Since the macroscopic elastic properties of membranes are a consequence of the molecular dynamics and packing, combined measurements of relaxation times and order parameters are well-suited to relate atomic-level properties to the macroscopic behavior of biological materials.

To understand the steeper slope and the bent shape of the square-law plots of the ras chains, we have determined order parameters and relaxation rates of DMPC-d_{54} in mixtures with cholesterol and the nonionic detergent $C_{12}E_8$. The values obtained are summarized in Table 3. Whereas cholesterol stiffens

Table 3. Segmental Order Parameters $|S_{CD}^{(i)}|$ and Spin−Lattice Relaxation Rates $R_{1Z}^{(i)}$ for DMPC-d_{54}/C$_{12}$E$_8$ and DMPC-d_{54}/Cholesterol Obtained at a Magnetic Field Strength of 17.6 T (115.1 MHz)

acyl chain segment	DMPC-d_{54}/C$_{12}$E$_8$[a,b]		acyl chain segment	DMPC-d_{54}/cholesterol[c]	
	$\|S_{CD}^{(i)}\|$	$R_{1Z}^{(i)}/s^{-1}$		$\|S_{CD}^{(i)}\|$	$R_{1Z}^{(i)}/s^{-1}$
			2−6	0.4344	17.62
			7	0.4031	17.59
2−8	0.1389	22.80	8	0.3306	13.58
9	0.1213	20.64	9	0.3181	12.20
10	0.0981	16.34	10	0.2745	11.99
11	0.0736	11.18	11	0.2495	12.27
12	0.0595	7.13	12	0.2004	10.73
13	0.0517	6.29	13	0.0632	4.75

[a] 40 °C; 90 wt % ${}^1H_2O$; 2:1 molar ratio. [b] Experimental values were obtained from magnetically oriented samples ($\theta = 90°$). [c] 30 °C; 50 wt % ${}^1H_2O$; 1:1 molar ratio.
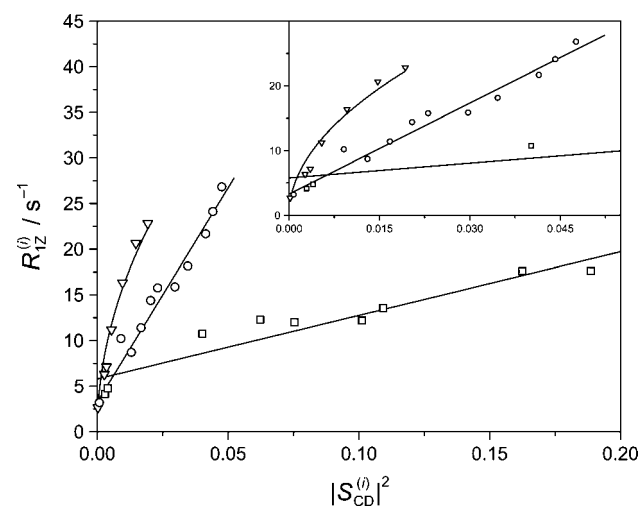

Figure 6. Plot of $R_{1Z}^{(i)}$ versus the square of the order parameter obtained at 115.1 MHz (17.6 T) showing the effect of membrane flexibility. Data are shown for DMPC-d_{54} (○) and DMPC-d_{54}/cholesterol (1:1 mol/mol) (□) at 30 °C and DMPC-d_{54}/C$_{12}$E$_8$ (2:1 mol/mol) at 40 °C (▽). The inset shows an expansion of the data for DMPC-d_{54} and DMPC-d_{54}/C$_{12}$E$_8$. The square-law plots can be used as a reference to estimate the flexibility of phospholipid membranes over relatively short distances approaching the molecular dimensions.

the membrane, addition of the detergent renders the membrane softer. These elastic properties should be visible in the in R_{1Z} versus $|S_{CD}|^2$ plots. Indeed, as shown in Figure 6, characteristic results are obtained for the respective samples, which confirm and extend previously published data.[36−38] The slope for the DMPC-d_{54}/cholesterol sample is much shallower compared to pure DMPC-d_{54}. By contrast the slope for the DMPC-d_{54}/C$_{12}$E$_8$ sample is steeper and the dependence is nonlinear. It is known that DMPC-d_{54} in the presence of cholesterol and at a temperature of 30 °C is in the liquid-ordered state.[50] This phase is characterized by a high order and a reduced segmental mobility concomitant with a reduction of the rate of *trans-gauche* isomerizations of the phospholipid chains. On the other hand, DMPC-d_{54} in the presence of $C_{12}E_8$ is known to have lower order parameters due to motions with larger amplitudes.[37,51,52] This seems to exactly describe the situation for the hydrocarbon

(50) (a) Vist, M. R.; Davis, J. H. *Biochemistry* **1990**, *29*, 451−464. (b) Thewalt, J. L.; Bloom, M. *Biophys. J.* **1992**, *63*, 1176−1181. (c) Ipsen, J. H.; Mouritsen, O. G.; Bloom, M. *Biophys. J.* **1990**, *57*, 405−412.
(51) Schneider, M. J.; Feller, S. E. *J. Phys. Chem. B* **2001**, *105*, 1331−1337.
(52) Klose, G.; Mädler, B.; Schäfer, H.; Schnier, K.-P. *J. Phys. Chem. B* **1999**, *103*, 3022−3029.

chains of the ras peptide in lipid membranes. Not only are the ras chains more loosely packed as expressed by low order parameters, they also appear to be highly flexible and dynamic, undergoing motions with large angular amplitudes. From the elasticity point of view, the lipid modifications of the ras peptide thus correspond to a soft and elastic material.

Discussion

The main goal of this study was to investigate the packing properties and dynamics of the lipid chain modifications of a membrane-bound lipidated ras peptide. In former research several spectroscopic techniques have been applied to obtain information on the structure, dynamics, and location of a lipidated heptapeptide comprising residues 180−186 of the C-terminus of N-ras in membranes consisting of dimyristoylphosphatidylcholine (DMPC).[26,48] The resulting model shows the ras peptide backbone to be at the lipid−water interface of the membrane, whereas the lipid modifications and hydrophobic amino acid side chains penetrate deeply into the hydrophobic core of the membrane. This model raises the question of how such an arrangement influences membrane packing properties. There is considerable interest in understanding the structural details of this membrane-binding mechanism of proteins involved in signal transduction events. This particularly concerns the molecular dynamics of the ras chains in comparison to the acyl chains of the host matrix.

From a physicochemical perspective it is known that each methylene segment of a hydrocarbon chain that partitions into a membrane contributes −3.45 kJ/mol to the binding energy.[15,17,18,53] For a single acyl chain, a unitary Gibbs free energy for partitioning into *n*-heptane of $\Delta G° = (17.81 - 3.45n_C)$ kJ/mol has been determined.[53] Thus, a significant membrane binding energy of almost −70 kJ/mol arises from the two hexadecyl chains covalently attached to the ras peptide. Despite this large favorable energy for chain partitioning, the binding energy of the entire protein is significantly lower. For instance, an entropy price must be paid when the ras peptide binds to the membrane since it loses translational and rotational degrees of freedom.[18] It has been estimated that only about 20% of singly palmitoylated protein molecules would be associated with the membrane, explaining the necessity of the second lipid modification for stable membrane binding.[17] In addition, the lipid membranes are in a fluid state, which means that the acyl chains of these molecules undergo rapid isomerizations, large amplitude motions, and changes between a huge number of conformational states.[32,54,55] Moreover, chain upturns and backfolding have been observed in these systems as a relatively common feature.[54,56] These effects due to the thermal energy of the system lead to a roughness of the membrane surface with a broad lipid water interface that occupies about half of the membrane thickness[57] and might be important for the question why singly lipid modified proteins do not form a stable association with the membrane. In consequence, there is an intriguing opposition

between the atomistic interactions that lead to the formation of these structures, the partitioning of the ras lipid chains, and the high molecular dynamics of the chains of the phospholipids and ras peptides forming the membrane.

Packing Properties of the ras Hydrocarbon Chains in a DMPC Matrix. The significant differences in chain order observed between the ras hydrocarbon chains and the phospholipid acyl chains provide a basis for understanding binding of the ras peptide to phospholipid membranes. Using a recently derived model that applies a potential of mean torque to relate molecular order parameters with hydrocarbon thickness, chain lengths, and areas,[33] we have shown that the ras hydrocarbon chains and the phospholipid acyl chains almost perfectly match in their length. This is in excellent agreement with a former investigation on the same peptide, where ^{1}H magic-angle spinning nuclear Overhauser enhancement spectroscopy and neutron diffraction methods were applied to localize the ras peptide in the lipid water interface of the phospholipid membrane.[26] Therefore, if the peptide backbone is inserted approximately at the level of the lipid glycerol backbone, one would assume that the peptide hydrocarbon chains would adopt a length very similar to that of the phospholipid acyl chains. This has been suggested on the basis of the diamond-lattice model,[58] which was applied to calculate the hydrocarbon thickness.[26] Molecular dynamics simulations using the same peptide and lipid matrix support our experimental findings.[59]

In addition to the hydrocarbon thickness we have calculated chain extension profiles for both the ras and the DMPC chains. For the ras peptide the distance between the terminal methylene group and the C-2 group is only 0.2 Å smaller than that for DMPC. Despite this small difference, the similarity between the ras and DMPC hydrocarbon chain length is evident and somewhat unexpected, since a ras hydrocarbon chain contains two additional methylene groups compared to the DMPC chains. As a result, the similarity in the projected chain lengths of the ras peptide and DMPC necessitates the low order parameters of the ras hydrocarbon chain in the DMPC matrix. If one assumes that the terminal methyl groups of the hydrocarbon chains of DMPC and ras are on average located at the same *z*-coordinate, a location of the peptide backbone in the lipid/water interface of the membrane can be concluded, which has indeed been determined previously.[26]

Considering the significant differences in packing between the DMPC acyl chains and ras hydrocarbon chains, the question about the biological significance of the disaturated lipid matrix for the insertion of lipidated peptides arises. Typically, biological membranes are composed of lipids with longer acyl chains (16 or 18 carbons) and varying degrees of unsaturation. In this regard, POPC is considered as a more relevant phospholipid, in comparison to DMPC, as its chain length is about 1.4 Å longer. However, due to the long measuring times required for the determination of the relaxation times of the ras peptide, we decided to use a DMPC matrix, which is more stable and not

(53) Tanford, C. *The Hydrophobic Effect: Formation of Micelles and Biological Membranes*; John Wiley & Sons: New York, 1980.

(54) Huster, D.; Arnold, K.; Gawrisch, K. *J. Phys. Chem. B* **1999**, *103*, 243−251.

(55) Petrache, H. I.; Gouliaev, N.; Tristram-Nagle, S.; Zhang, R.; Suter, R. M.; Nagle, J. F. *Phys. Rev. E.* **1998**, *57*, 7014−7024.

(56) (a) Huster, D.; Gawrisch, K. In *Lipid Bilayers: Structure and Interactions*; Katsaras, J., Gutberlet, T., Eds. Springer-Verlag: Berlin, 2000; pp 109−125. (b) Huster, D.; Gawrisch, K. *J. Am. Chem. Soc.* **1999**, *121*, 1992−1993.

(57) (a) White, S. H.; Ladokhin, A. S.; Jayasinghe, S.; Hristova, K. *J. Biol. Chem.* **2001**, *276*, 32395−32398. (b) White, S. H.; Wiener, M. C. In *Biological Membranes. A Molecular Perspective from Computation and Experiment*; Merz, K. M., Roux, B., Eds.; Birkhäuser: Boston, 1996; pp 127−144.

(58) Nagle, J. F. *Biophys. J.* **1993**, *64*, 1476−1481.

(59) (a) Gorfe, A. A.; Pellarin, R.; Caflisch, A. *J. Am. Chem. Soc.* **2004**, *126*, 15277−15286. (b) Feller, S. E., Vogel, A., Waldmann, H., Arnold, K., Huster, D. *Biophys. J.* **2005**, *88*, 422A.

prone to acyl chain hydrolysis or oxidation. Also, DMPC can be investigated in the liquid−crystalline phase state at 30 °C as opposed for instance to DPPC, which has its phase transition at about 41 °C.

Based on the results of ^{2}H solid-state NMR spectroscopy the ras hydrocarbon chains occupy a combined cross-sectional area of 67 Å^2 in the membrane. Since the backbone of the ras peptide is localized in the lipid water interface of the membrane,[26] the peptide backbone must cover the area of its chains to avoid exposure of the hydrocarbon interior of the membrane to the aqueous phase. To understand this issue it is useful to estimate the area that the peptide backbone occupies in the membrane. To this end, we have estimated the surface area of the peptide backbone to be roughly about 130 Å^2 by approximating it as a cylinder, which seems to be a fair approximation regarding the data of other experimental and computational studies.[26,59,60] This value is appreciably higher than the interfacial area of the two peptide hydrocarbon chains. However, the hydrophobic side chains of the ras peptide also insert into the membrane thereby occupying an additional cross-sectional area. It follows that the peptide backbone covers the hydrocarbon interior of the membrane but at the same time arranges itself at the lipid−water interface such that the packing of the DMPC host matrix is barely influenced. This would be in agreement with the experimental observation[48] that the ras peptide backbone does not form a secondary structure but remains flexible and can thus be located at the lipid−water interface without influencing the packing properties of the membrane.

Dynamic Properties of the ras Hydrocarbon Chains in a DMPC Matrix. Besides helping to understand the packing properties of the hydrocarbon chains, ^{2}H solid-state NMR provides further insight into the molecular dynamics of the various chain segments by relaxation measurements. The spin system relaxes to equilibrium by stochastic processes on the molecular level, such as internal motions, molecular reorientations, or bilayer collective deformations. Measurements of anisotropic ^{2}H relaxation rates have significantly contributed to the understanding of fluid membranes.[32,34,35,61,62] The analysis of the angular-dependent relaxation rates of the ras peptide is the subject of ongoing research in our laboratories. In this work, the spin−lattice relaxation rates of randomly oriented powder-type samples of ras-d_{66} and the DMPC-d_{54} host matrix are studied. From the R_{1Z} spin−lattice relaxation rates of the powder-type samples alone, comprehensive information about the molecular dynamics of the hydrocarbon chains requires the introduction of motional models for hydrocarbon chains containing several parameters that can only be determined by acquiring extensive sets of experimental data.[34] Nevertheless, by correlating the spin−lattice relaxation rates with the segmental order parameters, important information about molecular dynamics can be obtained. It has been shown that R_{1Z} versus $|S_{CD}|^2$ plots are a sensitive measure for the elastic properties of phospholipid membranes over relatively short time scales by combining packing properties with dynamic properties.[37−39]

Our work has uncovered significant differences between the elastic properties of the chains of the DMPC host matrix and the ras hydrocarbon chains. While the elastic properties of DMPC are only insignificantly altered by the presence of ras,

a completely different picture is obtained for the hydrocarbon chains of the ras peptide. The dynamic properties of the ras hydrocarbon chains in fact resemble those of phospholipid chains at high concentrations of detergents in the membrane. In the presence of detergents, membranes increase their softness, which is brought about by very flexible and mobile acyl chains characterized by low order parameters and large amplitude motions.[36,52] This leads to the important conclusion that the ras hydrocarbon chains that insert into the bilayer and attach the protein to the membrane surface are characterized by a high amount of flexibility. The question then arises of whether a more rigid arrangement of the ras chains would not provide a more stable chain insertion and anchoring of the ras peptide to the membrane. From our data alone, this question cannot be completely answered; however such a highly flexible arrangement of the hydrocarbon chains in the membrane may provide several important advantages for inserting a lipidated peptide into membranes.

Order fluctuations, meaning modulation of the local order parameter by slower motions, can in principle originate from collective motions of the acyl segments or motions of the molecular center of mass. Generally, either could give rise to a squared dependence of the relaxation rates on the local order parameter, which would be a square law if the amplitude is the same along the entire chain.[37] However, if the motions are more global as we propose here then the question arises as to why the relaxation rates of the peptide chains and the host matrix are not identical. From our data and molecular dynamics simulations (Scott Feller, unpublished results) we can clearly exclude the influence of geometrical contributions to the low order parameters of the ras chains.

The ^{2}H NMR data show that the host DMPC chains are only slightly affected by the ras peptide, whereas the ras peptide chains evince a high degree of flexibility. The DMPC chains are in a fluidlike bilayer environment whose elasticity is approximately the same as that in the absence of ras peptide. By contrast, if the ras peptide chains are observed directly with ^{2}H NMR, they appear to be in a microenvironment similar to phospholipids in the presence of a high amount of detergent. These observations can be simply explained in terms of two environments within the bilayer, one corresponding to the bulk bilayer lipids and the other representing microdomains with the ras peptide. The host DMPC component is free to exchange between the bulk bilayer and the ras peptide microdomains on the ^{2}H NMR time scale ($\sim10^{-5}$ s). On the other hand, the ras peptide is confined to microdomains which include a small number of DMPC chains exchanging with the bulk lipids as indicated above. The presence of two different types of chains is analogous to mixed chain phospholipid systems, e.g., phospholipids containing detergents[36] or mixed-chain saturated-polyunsaturated bilayers.[63] An enhanced flexibility within the microdomains is manifested by the square-law plots. In addition, the ras peptide is larger than a lipid and has a different shape with a larger moment of inertia. The molecular contribution may be larger for the ras peptide chains since they pick up the slower motions of the entire molecule. Influences of relatively slow

(60) Zamyatin, A. A. *Prog. Biophys. Mol. Biol.* **1972**, *24*, 107−123.

(61) Jarrell, H. C.; Smith, C. P.; Jovall, P. A.; Mantsch, H. H.; Siminovitch, D. J. *J. Chem. Phys.* **1988**, *88*, 1260−1263.
(62) Meier, P.; Ohmes, E.; Kothe, G. *J. Chem. Phys.* **1986**, *85*, 3598−3614.
(63) (a) Petrache, H. I.; Salmon, A.; Brown, M. F. *J. Am. Chem. Soc.* **2001**, *123*, 12611−12622. (b) Rajamoorthi, K.; Petrache, H. I.; McIntosh, T. J.; Brown, M. F. *J. Am. Chem. Soc.* **2005**, *127*, 1576−1588.

motions of the entire ras peptide molecule may thus provide an additional contribution to R_{1Z}, which would be superimposed on the collective disturbances of its microenvironment.

Regarding the biological significance of our findings, we note that the flexible peptide hydrocarbon chains can most easily insert into a fluid membrane that is characterized by a large amount of molecular disorder. Instead of the membrane adjusting to a rigid molecule by local curvature, which costs free energy, the peptide chains insert into the hydrophobic membrane interior with almost no energy cost, thereby increasing their configurational entropy and leaving the host matrix largely unchanged. This is in contrast to other lipidated proteins that bind to the membrane by a combination of electrostatic and hydrophobic interactions, such as K-ras, Src, NAP-22, or MARCKS.[14,64−66] For stable membrane insertion, these proteins require one myristoyl lipid modification and a nearby cluster of basic amino acids that interact with the negatively charged cytosolic membrane surface.[15,67] From model studies it has been estimated that about four methylene segments are localized in the aqueous environment because the neighboring basic residues are confined to the volume immediately above the membrane surface.[65] This energetically unfavorable scenario is possible since the Src peptide contains several positively charged residues in the direct vicinity of the myristoyl chain. Bringing these residues closer to the membrane surface would cost more energy (due to Born repulsion) than exposing four methylenes to the water. The ras peptide does not contain charged amino acids but some rather hydrophobic residues instead (1 Leu, 1 Met).

This would suggest that these side chains insert into the membrane and drag the peptide backbone into the lipid−water interface of the bilayer.

One should also recall that the flexible ras hydrocarbon chains occupy a rather substantial cross-sectional area in the membrane that needs to be covered by the polypeptide backbone. Thus, the peptide backbone can penetrate the membrane and insert into the lipid−water interface of the bilayer. In this way not only the hydrocarbon chains are inserted into the membrane interior but also the hydrophobic side chains such as Met and Leu can contribute to the binding energy, which has been found experimentally.[26] Evidently the dynamic and flexible arrangement of the hydrocarbon chains of the lipidated ras peptide may represent a specific requirement for the interaction with other proteins such as palmitoyltransferases that regulate membrane binding and desorption. Clearly, much more work is required to fully understand these structurally and functionally important questions regarding the binding mechanism of lipid modified peptides and proteins. Besides experimental work, further detailed insight is possible by conducting molecular dynamics simulations in conjunction with the packing parameters derived in this study. Such studies are currently in progress.

Supporting Information Available: Details about the ras peptide synthesis and analytical characterization are provided. This material is available free of charge via the Internet at http://pubs.acs.org.

JA051856C

(64) (a) Qin, Z.; Cafiso, D. S. *Biochemistry* **1996**, *35*, 2917−2925. (b) Arbuzova, A.; Wang, J.; Murray, D.; Jacob, J.; Cafiso, D. S.; McLaughlin, S. *J. Biol. Chem.* **1997**, *272*, 27167−27177.
(65) Murray, D.; Hermida-Matsumoto, L.; Buser, C. A.; Tsang, J.; Sigal, C. T.; Ben-Tal, N.; Honig, B.; Resh, M. D.; McLaughlin, S. *Biochemistry* **1998**, *37*, 2145−2159.
(66) (a) Khan, T. K.; Yang, B.; Thompson, N. L.; Maekawa, S.; Epand, R. M.; Jacobson, K. *Biochemistry* **2003**, *42*, 4780−4786. (b) Epand, R. M.; Maekawa, S.; Yip, C. M.; Epand, R. F. *Biochemistry* **2001**, *40*, 10514−10521.
(67) McLaughlin, S.; Aderem, A. *Trends Biochem. Sci.* **1995**, *20*, 272−276.